| REPORT DOCUMENTATION PAGE | | READ INSTRUCTIONS BEFORE COMPLETING FORM |
|---|---|---|
| 1. REPORT NUMBER<br>Technical Report No. 1  1980-81 | 2. GOVT ACCESSION NO.<br>AD-A109 15? | 3. RECIPIENT'S CATALOG NUMBER |
| 4. TITLE (and Subtitle)<br>"Grain-Coarsening Resistance and the Stability of Second-Phase Dispersions in Rapidly Solidified Steels" | | 5. TYPE OF REPORT & PERIOD COVERED<br>Technical; Oct. 1980 – Sept. 1981 |
| | | 6. PERFORMING ORG. REPORT NUMBER |
| 7. AUTHOR(s)<br>G. B. Olson, H. C. Ling*, J. S. Montgomery, J. B. Vander Sande, and M. Cohen | | 8. CONTRACT OR GRANT NUMBER(s)<br>N00014-81-K-0013 |
| 9. PERFORMING ORGANIZATION NAME AND ADDRESS<br>Massachusetts Institute of Technology<br>Cambridge, MA 02139 | | 10. PROGRAM ELEMENT, PROJECT, TASK AREA & WORK UNIT NUMBERS |
| 11. CONTROLLING OFFICE NAME AND ADDRESS<br>Office of Naval Research<br>Arlington, VA 22217 | | 12. REPORT DATE<br>1 December 1981 |
| | | 13. NUMBER OF PAGES<br>8 |
| 14. MONITORING AGENCY NAME & ADDRESS(if different from Controlling Office) | | 15. SECURITY CLASS. (of this report)<br>Unclassified |
| | | 15a. DECLASSIFICATION/DOWNGRADING SCHEDULE |

**LEVEL**

16. DISTRIBUTION STATEMENT (of this Report)

Unlimited.

17. DISTRIBUTION STATEMENT (of the abstract entered in Block 20, if different from Report)

19. KEY WORDS (Continue on reverse side if necessary and identify by block number)

Rapid solidification, grain growth, phase stability

20. ABSTRACT (Continue on reverse side if necessary and identify by block number)
Control of alloy composition and processing to achieve grain coarsening resistance in rapidly solidified alloys is examined via the theory of grain boundary pinning and particle coarsening. The principles are illustrated for the case of manganese sulfides in steels. A thermodynamic survey of potential stable dispersed phases identifies TiN and rare-earth sulfides as particularly promising for alloy development via rapid solidification.

DD FORM 1473 EDITION OF 1 NOV 65 IS OBSOLETE
S/N 0102-014-6601

*Allied Chemical Corporation, Morristown,

# GRAIN-COARSENING RESISTANCE AND THE STABILITY OF SECOND-PHASE DISPERSIONS IN RAPIDLY SOLIDIFIED STEELS

G. B. OLSON, H. C. LING*, J. S. MONTGOMERY, J. B. VANDER SANDE, AND M. COHEN
MIT, Cambridge, MA; *now at Western Electric Engineering Research Labs.,
Princeton, NJ, USA

## ABSTRACT

Control of alloy composition and processing to achieve
grain coarsening resistance in rapidly solidified alloys
is examined via the theory of grain boundary pinning and
particle coarsening. The principles are illustrated for
the case of manganese sulfides in steels. A thermodynamic
survey of potential stable dispersed phases identifies TiN
and rare-earth sulfides as particularly promising for alloy
development via rapid solidification.

## INTRODUCTION

An investigation of the tempering and grain growth behavior of rapidly solidi-
fied Ni-Co and Mo steels has revealed a remarkable resistance to high tempera-
ture grain coarsening [1]. At 1200C where conventionally processed steels
coarsen to austenitic grain sizes of several hundred microns, the rapidly solidi-
fied (RSP) steels retain a grain size of 10-20 $\mu m$. Electron microscopy suggests
that the coarsening resistance is due to finely dispersed stable inclusions,
principally sulfides, which can maintain a ~0.1 $\mu m$ particle size during high
temperature austenitizing. This coarsening resistance is of potential benefit
to the mechanical properties of steels for which high austenitizing temperatures
have been found to improve sharp-crack fracture toughness ($K_{IC}$) but with losses
in other fracture properties associated with grain coarsening. Preliminary
toughness measurements on the rapidly solidified steels have revealed $K_{IC}$ values
equal to or superior to conventionally processed material, and substantial in-
creases with high austenitizing treatments have been obtained without dele-
terious grain coarsening [2].

In view of the potential importance of this phenomenon, the control of boun-
dary pinning dispersions is here assessed in light of the theory of grain
boundary pinning and particle coarsening, and the relative thermodynamic stabili-
ty of potential dispersed phases in steels is surveyed to provide alloy design
guidelines for rapid solidification processing.

## GRAIN BOUNDARY PINNING AND PARTICLE COARSENING

Several detailed treatments [3-5] have extended the original model of Zener
[6] for the pinning effect of second-phase particles on grain boundaries. These
models can be used to predict a limiting grain size at which the driving force
for grain growth is balanced by the particle pinning force. The model of
Gladman [3], which has been quantitatively applied to the grain coarsening of
austenite [7], predicts a limiting grain size expressed by:

$$2R = \frac{\pi}{3} \frac{\bar{r}}{f_v} \left(\frac{3}{2} - \frac{2}{Z}\right), \tag{1}$$

where R is the limiting grain radius, $\bar{r}$ is the mean particle radius, $f_v$

the particle volume fraction, and Z is a grain size distribution parameter
(ratio of the largest to the average grain size) determining the driving force
for grain growth. As in all such pinning models, the limiting grain size is
proportional to $\bar{r}$ and inversely proportional to $f_v$. For a given $f_v$, then,
grain size is minimized by finely dispersing the pinning particles (reducing $\bar{r}$),
and grain growth governed by this force balance will be controlled by the par-
ticle coarsening behavior which then controls $\bar{r}$.

For the case of small $f_v$ and uniform dispersions, the volume-diffusion con-
trolled coarsening of second-phase particles can be adequately treated by the
Lifshitz-Slyozov-Wagner (LSW) theory [8,9], as applied to the case of binary
compounds in a matrix of a third element by Bhattacharyya and Russell [10]:

$$\bar{r}^3 - \bar{r}_0^{\,3} = \frac{8}{9} \frac{DC}{R_g T} \; \sigma \, V_p^{\,2} t. \tag{2}$$

Here, $\bar{r}_0$ is the initial particle radius, D and C are the diffusivity and con-
centration in solution of the rate-controlling species, $R_g$ the gas constant,
T the absolute temperature, $\sigma$ the particle surface energy, $V_p$ the particle
molar volume, and t the heat treatment time. The rate controlling species is
that for which the product DC is smallest.

A recent study of particle coarsening in rapidly solidified aluminum alloys
[11] indicates that accelerated boundary-diffusion controlled coarsening can be
important at lower temperatures, but that the volume-diffusion controlled be-
havior of equation 2 obtains in the higher temperature regime of interest here.
Combining equations 1 and 2 then predicts a $t^{1/3}$ time dependence for particle-
pinning controlled grain coarsening.

Considering a compound precipitate of the form MX and expressing the wt.%
contents of each element as M and X with [M] and [X] the wt.% concentrations in
solution, the volume fraction of precipitate and concentrations in solution can
be expressed by:

$$f_v = \frac{1}{100} \; \frac{\rho_m}{\rho_p} \; (\frac{A_M + A_X}{2})(\frac{X}{A_X} + \frac{M}{A_M})\phi \tag{3a}$$

$$[M] = M - \frac{A_M}{2} \; (\frac{X}{A_X} + \frac{M}{A_M}) \; \phi \tag{3b}$$

$$[X] = X - \frac{A_X}{2} (\frac{X}{A_X} + \frac{M}{A_M}) \; \phi \tag{3c}$$

$$\text{where } \phi = 1 - [1 - \frac{4 \, A_M A_X}{(MA_X + XA_M)^2} \; (MX - K_S)]^{1/2} . \tag{3d}$$

Here, $\rho_m$ and $\rho_p$ are the matrix and particle densities, $A_M$ and $A_X$ are the atomic
weights of M and X, and $K_S$ is the equilibrium solubility product for the MX
compound expressed by:

$$K_S = [M][X] = K_0 \exp(-H/R_g T), \tag{4}$$

with H the heat of solution and $K_0$ a constant. Concentrations in solution can
be converted to the appropriate units (moles/volume) for equation 2 by the
relations:

$$C_M = \frac{[M]}{100 \, V_m} \frac{A_m}{A_M} , \qquad C_X = \frac{[X]}{100 \, V_m} \frac{A_m}{A_X} , \tag{5}$$
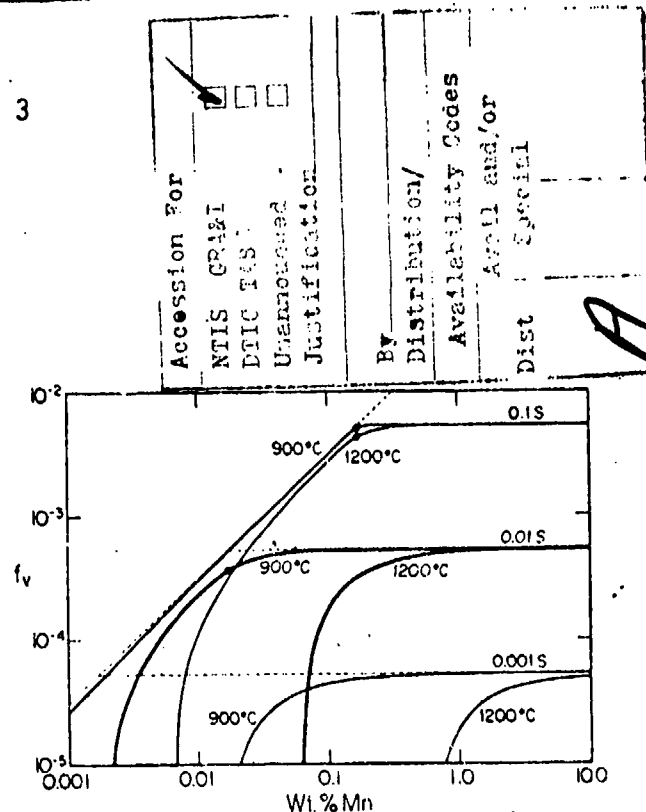
3



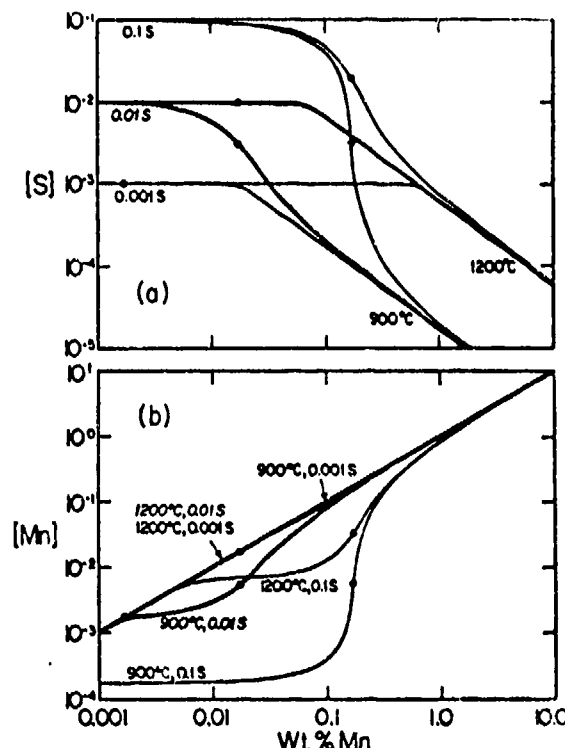Fig. 1. Volume fraction, $f_v$, of MnS vs. alloy Mn content for three S levels at 900C and 1200C.

Fig. 2. Concentrations of S and Mn in solution.

with $V_m$ and $A_m$ the molar volume and atomic weight of the matrix. Equations 3a-d show that for a given alloy composition, $f_v$ is increased and [M] and [X] are decreased, promoting boundary pinning and low-particle coarsening, if the solubility product $K_s$ is small. Further analysis shows that, for a given composition product MX, $f_v$ is maximized when the ratio of M to X is that of the particle stoichiometry. Another property of compositions in the stoichiometric ratio is that $C_M$ and $C_X$ are then equal which guarantees coarsening rate control by the slower diffusing species via the DC product in equation 2. These features are illustrated in further detail for the case of MnS in austenitic iron in Figures 1 to 4.

Figure 1 shows the calculated volume fraction of sulfides versus alloy manganese content for three sulfur levels (in wt.%) at 900 and 1200C based on available solubility data [12]. If MnS were completely insoluble, $f_v$ would follow the dashed diagonal line until all the sulfur was removed from solution as represented by the dashed horizontal lines. The actual temperature-dependent solubility gives the behavior depicted by the solid curves. Heavy points correspond to the stoichiometric ratio compositions. The heavy curves represent a typical sulfur content of 0.01 wt.% for commercial steels, for which it is seen that an $f_v$ of ~0.1% is maintained at 1200C over the typical composition range of 0.2 to 1.0 wt.% Mn.

Corresponding matrix concentrations of S and Mn are presented in Figure 2, showing the general decrease of [S] and increase of [Mn] with alloy Mn content. At alloy compositions high enough to exceed the solubility product, as represented by the 0.1S curves, maximum rates of decrease of [S] and increase of [Mn] occur at the stoichiometric ratio compositions marked by the heavy points. At lower S contents the [S] curves flatten and [Mn] curves become linear when complete dissolution of MnS occurs.

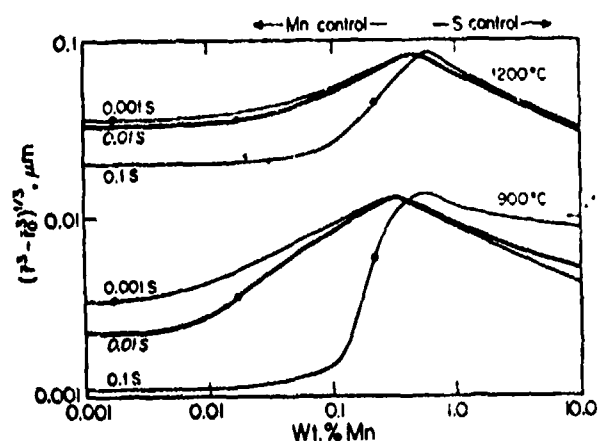Using available diffusivity data for Mn and S in austenite [13,14], taking

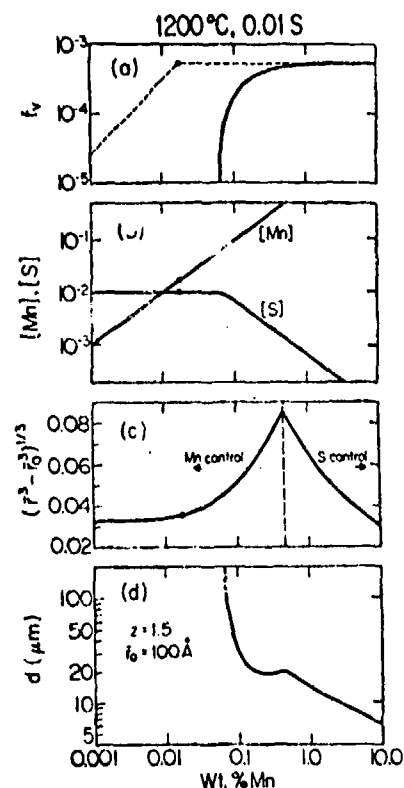Fig. 3. Calculated MnS coarsening increment for one hour at 900C and 1200C.

Fig. 4. Summary plot for 0.01S at 1200C including linear intercept grain size in (d).

$\sigma \approx 1$ J/m$^2$, and incorporating the calculated matrix concentrations of Figure 2, particle coarsening increments for one-hour treatments according to equation 2 are shown in Figure 3. The maximum coarsening, which occurs at the boundary between Mn and S diffusion control, is insensitive to S content and occurs right in the range of Mn contents of commercial steels. The coarsening increases by an order of magnitude going from 900 to 1200C. Coarsening can be significantly decreased using the stoichiometric compositions (heavy points) for which Mn diffusion controls, but this is not practical in this particular case primarily due to the need for high Mn/S ratios to avoid low melting point iron sulfides and the undesirability of S in solution due to its embrittling effect.

Results of these calculations for the case of 0.01S at 1200C are combined in Figure 4. Figure 4d shows the predicted linear intercept grain size from equation 1 using Z = 1.5 based on the austenite grain coarsening study of Gladman and Pickering [7] and taking $\bar{r}_0$ = 100 Å from observations on a rapidly solidified high-sulfur steel [15]. In spite of the coarsening peak in Figure 4c, the composition dependence of $f_v$ in Figure 4a gives a grain size of $\sim$20 µm which is fairly insensitive to Mn content over the commercial alloy range. At the sulfur content of 0.01S, use of a stoichiometric Mn content is not possible due to complete dissolution of the sulfides. Some improvement in grain refinement could be obtained by increasing Mn to $\sim$2%.

Defining a coarsening increment as $\delta = (\bar{r}^3 - \bar{r}_0^3)^{1/3}$, it can be seen that when $\bar{r}_0 > 2\delta$, $\bar{r}$ is dominated by the initial particle size, and when $\bar{r}_0 < \delta/2$, $\bar{r}$ is dominated by coarsening. Hence, for the $\delta$ associated with a given heat treatment, there is no advantage in making $\bar{r}_0$ any finer than $\delta/2$. For the coarsening increments of Figure 4c, the 100 Å particle radius that can be obtained by rapid solidification is sufficiently fine to take full advantage of the stability of MnS as a grain refining dispersion.
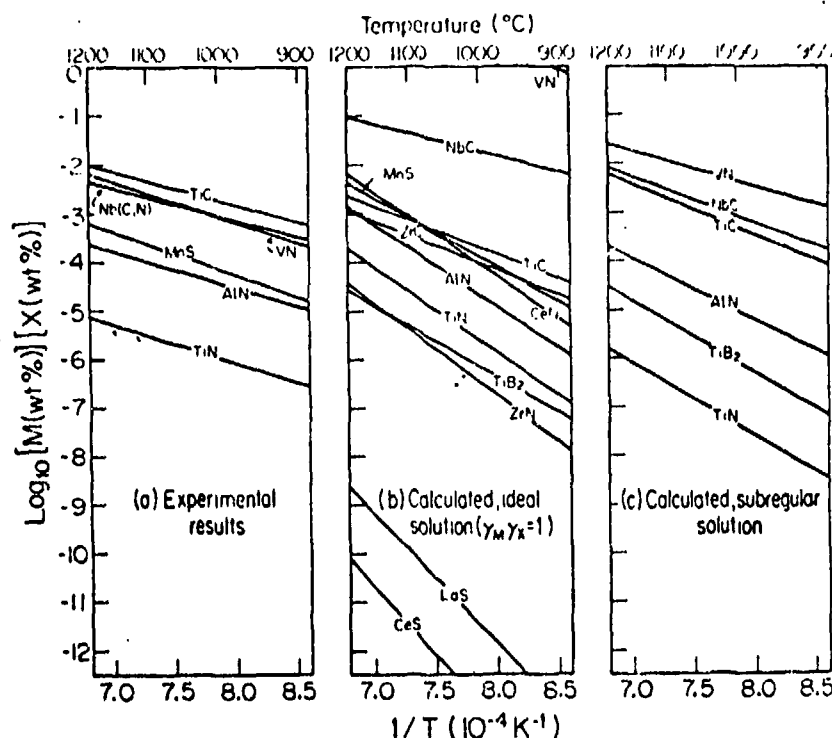
Fig. 5. Experimental and calculated solubility products for compounds in austenitic iron.

Further improvement in coarsening resistance could be obtained by dispersing more stable compounds. For example, substitution for Mn by a stronger sulfide former with a lower solubility product could move the $f_\gamma$ curve of Figure 4a to the left allowing use of a stoichiometric composition with reduced coarsening while also lowering [S]. To this end, the relative thermodynamic stability of potential dispersed phases in steels has been surveyed.

THERMODYNAMIC STABILITY OF COMPOUNDS IN STEELS

The equilibrium solubility product for an MX compound in an alloy can be derived from the relation

$$\ln \gamma_M c_M \gamma_X c_X = -\frac{\Delta G}{R_g T} , \qquad (6)$$

where $c_M$ and $c_X$ are the concentrations of M and X in solution (expressed as atom fractions), $\gamma_M$ and $\gamma_X$ are the activity coefficients of M and X, and $\Delta G$ is the free-energy of dissociation of MX. For dilute solutions, $\gamma_M$ and $\gamma_X$ are approximately constant (Henry's law) and equation 6 then leads to a composition independent solubility product of the form of equation 4.

Experimentally determined solubility products for relatively stable compounds in steels over the temperature range of 900 to 1200C are summarized in Figure 5a. Included are results for Nb(C,N) and AlN[7], MnS[12], VN and TiC [16], and TiN[17]. In order to explore further compounds for which experimental solubility data is not available, approximate solubility products were estimated from available thermochemical data for compound free-energies of formation [18-21] according to equation 6 adopting the assumption $\gamma_M \gamma_X = 1$ corresponding to an ideal solution. This gives the results presented in Figure 5b.

TABLE I
Solubility Products for Compounds in Austenite

| Compound | $\log_{10}$ [M,w/o][X, w/o] | |
| --- | --- | --- |
| | experiment | calculated |
| VN | -8330/T + 3.46 | -7242/T + 3.32 |
| NbC | -6770/T + 2.26 | -9516/T + 4.39 |
| TiC | -7000/T + 2.75 | -10470/T + 4.91 |
| MnS | -9020/T + 2.93 | - |
| AlN | -7500/T + 1.48 | -12882/T + 5.09 |
| TiB$_2$ | - | -14964/T + 5.67 |
| TiN | -8000/T + 0.32 | -14990/T + 4.39 |

While this approximation provides a rough guide to relative solubilities, direct comparisons in those cases where experimental information is available (e.g. TiC, MnS, AlN, TiN) shows significant discrepancies.

As a further refinement of the solubility calculations, available subregular solution model interaction parameters [22] were used to estimate activity coefficients for solutes in austenitic iron. As a more direct comparison with experiment, activities were estimated for the same C, Mn, and Si contents as for the steels on which the experimental data of Figure 5a were obtained. These results are summarized in Figure 5c and the temperature-dependent solubility products are compared against the experimental data in Table I. Allowing for the very approximate nature of the estimated interaction parameters for the case of VN, agreement between theory and experiment is excellent at high temperatures. The predictions for TiC and TiN are also in good agreement with a similar calculation by Hoch and Chen [23]. In general, the predicted slopes in Figure 5c are steeper than for the experimental data of Figure 5a. The experiments, in which alloys were cooled to temperature and held for only one hour, may overestimate solubilities at lower temperatures where equilibrium may not have been achieved.

Combining the information available from Figure 5 provides some guidance in the selection of dispersed phases in rapidly solidified steels. The experimental data of Figure 5a suggest that MnS is not intrinsically more stable than AlN; the higher relative stability indicated in rapidly solidified steels may be due to the greater Mn contents employed relative to typical Al contents. The calculations verify that TiB$_2$, which has been successfully used in rapidly solidified nickel-base alloys and some steels, is indeed quite stable, but it appears that TiN is even more stable. Also of interest, based on the ideal solution estimates of Figure 5b, are the extremely stable rare-earth sulfides which may exhibit sufficient solubility in the liquid to allow dispersion by rapid solidification if oxygen is held to low enough levels.

Efforts are underway to obtain stable grain refining dispersions of TiN in gas atomized microalloyed steels, and rare-earth sulfides in high-strength martensitic steels. The latter may allow the additional benefit of eliminating manganese from steels thereby improving resistance to stress corrosion and hydrogen embrittlement [24].

CONCLUSIONS

An extreme resistance to high temperature grain coarsening can be obtained by finely dispersing stable phases via rapid solidification. The highest coarsening resistance is obtained from compounds of the lowest solubility, precipitated from alloy compositions in the stoichiometric ratio of the compound. The most efficient dispersion involves an initial particle radius

equal to half the coarsening increment $(\bar{r}^3 - \bar{r}_0{}^3)^{1/3}$ for the desired heat treatment conditions. Finely dispersed manganese sulfides can provide exceptional grain coarsening resistance at 1200C in commercial steels, but several other compounds, most notably TiN and rare earth sulfides should be even more effective.

## ACKNOWLEDGMENTS

## REFERENCES

1.  M. Suga, J. L. Goss, G. B. Olson, and J. B. Vander Sande, Proc. 2nd Intl. Conf. Rapid Solidification Processing: Principles and Technologies (Claitor's, Baton Rouge, 1980) pp. 364-371.

2.  P. M. Fleyshman, M.I.T. Thesis research in progress.

3.  T. Gladman, Proc. Roy. Soc. A 294, 298 (1966).

4.  M. F. Ashby, J. Harper, and J. Lewis, Trans. AIME 245, 413 (1969).

5.  P. Hellman and M. Hillert, Scandinavian Journal of Metallurgy 4, 211 (1975).

6.  C. Zener, quoted by C. S. Smith, Trans. AIME 175 47 (1948).

7.  T. Gladman and F. B. Pickering, J. Iron Steel Inst. 205, 653 (1967).

8.  I. M. Lifshitz and V. V. Slyozov, J. Phys. Chem. Solids 19, 35 (1961).

9.  C. Wagner, Z. Elektrochem. 65, 581 (1961).

10. S. K. Bhattacharyya and K. C. Russell, Met. Trans. 3, 2195 (1972).

11. H. Jones, Proc. 2nd Intl. Conf. Rapid Solidification Processing: Principles and Technologies (Claitor's, Baton Rouge, 1980) pp. 306-316.

12. E. T. Turkdogan, S. Ignatowicz, and J. Pearson, J. Iron and Steel Inst. 180, 349 (1955).

13. A. F. Smith and R. Hales, Metal Science 9, 181 (1975).

14. M. A. Krishtal, Diffusion Processes in Iron Alloys, p. 177, trans. from Russian by A. Wald, ed. J. J. Becker, Israel Program for Federal Scientific Translations, available Clearinghouse for Federal Scientific and Technical Information, Springfield, VA (1970).

15. T. F. Kelly and J. B. Vander Sande, Proc. 2nd Intl. Conf. Rapid Solidification Processing: Principles and Technologies (Claitor's, Baton Rouge, 1980) pp. 100-111.

16. K. J. Irvine, F. B. Pickering, and T. Gladman, J. Iron and Steel Inst. 205, 161 (1967).

17. S. Matsuda and N. Okumura, "Tetsu-to-Hagane," J. Iron and Steel Inst. Japan 62, 1209 (1976).

18. J.A.N.A.F. Thermochemical Tables, 2nd ed. (1970).

19. O. Kuraschewski and C. B. Alcock, Metallurgical Thermochemistry, 5th ed. (Pergamon, NY, 1979).

20. J. F. Elliott, M. Gleiser, and V. Ramakrishna, Thermochemistry for Steel-making Vol. II (Addison-Wesley, MA, 1963).

21. W. G. Wilson, D. A. R. Kay, and A. Vahed, J. Metals, May 1974, p. 14.

22. Manlabs-NPL Thermochemical Databank.

23. M. Hoch and Y. S. Chen, in The Industrial Use of Thermochemical Data p. 312.

24. S. K. Banerji, C. J. McMahon, and H. C. Feng, Met. Trans. 9A, 237 (1978).